Bitlis Eren Üniversitesi Fen Bilimleri Dergisi
BİTLİS EREN UNIVERSITY JOURNAL OF SCIENCE
ISSN: 2147-3129/e-ISSN: 2147-3188
VOLUME: 12 NO: 3 PAGE: 925-940 YEAR: 2023
DOI:10.17798/bitlisfen.1346730

3BResNet: A Novel Residual Block-Based ResNet Model Approach for COVID19 Detection

Ekrem Eşref KILINÇ[1*], Fahrettin AKA[2], Sedat METLEK[3]

[1]*Burdur Mehmet Akif Ersoy University, Vocational School of Ağlasun, Department of Computer Technology and Programming, Burdur / Türkiye*
[2]*Isparta University of Applied Sciences, Vocational School of Atabey, Department of Computer Technologies, Isparta / Türkiye*
[3]*Burdur Mehmet Akif Ersoy University, Vocational School of Technical Sciences, Department of Electronics and Automation, Burdur / Türkiye*
(ORCID: 0000-0003-1806-4937) (ORCID: 0000-0003-1449-2969) (ORCID: 0000-0002-0393-9908)

Keywords: Deep Neural Network, Residual Block, Resnet, 3BResNet.

Abstract

In recent years, upper respiratory tract infections that have affected the whole world have caused the death of millions of people. It is predicted that similar infections may occur in the coming years. Therefore, it is necessary to develop methods that can be used widely, especially during epidemic periods. The study developed a decision support system for use in upper respiratory tract infections. At this stage, first, the ResNet models in the literature were examined and an application was developed on the SARS-CoV-2 Ct dataset. Next stage, the block structure in the ResNet models in the literature was changed, the number of layers was reduced, and a new model was proposed that provides higher success with fewer parameters. With the proposed model, the values 0.97, 0.97, 0.94, and 0.98 were achieved for accuracy, F1 score, precision and sensitivity on the SARS-CoV-2 Ct dataset, respectively. When the obtained values are compared to state of the art methods in the literature, it has been determined that they are at a competitive level with much fewer parameters. Hardware-related problems encountered in the training of ResNet models at low hardware levels were solved with the proposed model, resulting in a higher success rate. Furthermore, the proposed model can be widely used in different decision support systems that are urgently needed in adverse conditions such as pandemics due to its lightweight structure and high-performance results. As a result of the study, a new model that can provide higher performance with much lower layer structure than existing ResNet models has been introduced into the literature with the proposed model.

1. Introduction

The easy transmission of upper respiratory tract diseases causes regional or worldwide outbreaks. Recently, one of these epidemics emerged in the city of Wuhan, China and affected the whole world [1]. As a result, the World Health Organization (WHO) announced this situation as a pandemic due to the risk of spreading the disease easily to the masses [2]. During the pandemic, the authorities reported about 600 million cases and about 7 million deaths [3].

Due to the deaths that occurred during the pandemic period, health facilities such as emergency rooms and intensive care units were also overcrowded. This situation caused significant labor and financial difficulties [4]. In order to prevent these difficulties at least one step, it has become an extremely vital issue to detect diseases that may pose a risk of epidemic and to take the necessary precautions. For this reason, many studies have been conducted in the literature to detect disease [5]. One of the most fundamental studies is the Real-Time

*Corresponding author: ekilinc@mehmetakif.edu.tr
Received: 21.08.2023, Accepted: 16.09.2023

Polymerase Chain Reaction (RT-PCR) method [6]. Thanks to the RT-PCR method, which was used extensively during the Covid19 pandemic period, numerous patients were diagnosed with the disease. However, one of the biggest obstacles to the efficient use of the system is that the method used gives results after a long time. In addition, some inconsistencies in the results of RT-PCR testing have called into question the reliability of this method. Despite the disadvantages of this method, it was the most preferred method because there were not many alternatives during the pandemic. However, delivering diagnostic test kits using the RT-PCR method over a wide geographic area during the pandemic period presented a different problem.

The use of technology to provide diagnosis and treatment to large populations is critical during such epidemics. Therefore, researchers have focused on rapid response systems as an alternative to test kits in disease diagnosis [7]. Radiological images are one of the most important of these. Radiological images are used in the detection of many diseases because they can be easily obtained from X-ray machines commonly found in hospitals [8]. However, since the soft tissues cannot be fully detected with X-ray images, Computed Tomography (CT) scans, which give faster results, are preferred [9]. This method was preferred because it is both safer and gives faster results than other test kits. It is considered a safer method than many other diagnostic methods, especially when evaluated in terms of maintaining physical distance between the patient and the doctor. Machine learning methods that use CT images for faster and more reliable disease detection have also begun to be developed. One of the leading machine learning methods is deep learning (DL) algorithms. Ancillary decision support systems created with DL algorithms can help experts make more accurate decisions faster [10]. Transfer learning methods are at the forefront of DL algorithms that are commonly used in auxiliary decision support systems. Transfer learning methods are based on using the weight values of pre-trained models on new datasets. This approach greatly decreases the training time for models and simplifies the determination of weight values for the layers utilized in deep neural network models [11].

In the literature, it is claimed that models based on the transfer learning method give better results than basic convolutional neural networks (CNN) or other machine learning models in classifying images in datasets consisting of medical images [12]. For this reason, numerous research studies in the literature employ transfer learning techniques to train neural network models on limited-sized datasets [13] – [16].

Studies that use DL methods and CT images together for disease detection are commonly found in the literature. Residual Network (ResNet) based methods are used in many of these studies. But in general, ResNet-based models have some disadvantages. There are several gaps in the literature that need to be filled to overcome these disadvantages. The major gaps identified in the literature are:

- At higher depth levels, semantic gaps occur. The most important factor that causes this semantic gap is the vanishing or exploding. Although increasing the number of layers in ResNet models is done to improve performance, this can produce low-performance results depending on the dataset. For this reason, when reviewing the studies in the literature, it is generally found that different ResNet models produce more successful results on different datasets. This situation can lead to problems concerning the comparison of ResNet models.
- In the literature, a limited number of ResNet models and different models are compared on the same dataset in studies conducted to measure the performance of ResNet models. The datasets used in these studies are generally datasets with access problems [17]. For this reason, it is necessary to carry out new studies in which ResNet models will be compared with each other using publicly available datasets.
- The process of transferring filters obtained from a pre-trained model to a new model is called transfer learning. This method allows the model to be trained quickly and allows for better results. In addition, when randomly selected filters are used for training, the time required for training the models increases excessively. In this case, training can take days, especially when training is done on a low-equipped level. Therefore, new solutions are needed that can be trained and operated in low-equipped systems are needed.

To fill the similar gaps mentioned in the literature, a study was conducted to categorize patients infected with Covid19 using different ResNet models on the publicly accessible dataset "The severe acute respiratory syndrome coronavirus 2 (SARS-CoV-2) Ct-Scan". A novel approach is presented, utilizing convolutional and residual blocks, which eliminates the disadvantages of ResNet models for the classification of individuals with Covid19 infection. The study's contribution to the literature is briefly summarized below.

- In the proposed model (3BResNet), a competitive alternative has been developed that can operate on platforms with lower hardware capacity by reducing the layer count, the parameter count, and the computational cost.
- A different residual block structure has been developed for the issue of overfitting, which is the primary problem of ResNet models. The developed structure has been used in the 3BResNet model and compared with other ResNet models in the literature.
- The block structure used in the ResNet18, ResNet34, ResNet50, ResNet101, ResNet152, and ResNet202 models in the literature and the effect of the 3BResNet block structure on the model success are presented in detail in the study.
- In the study, instead of increasing the number of layers as in ResNet models, it has been determined that the use of the proposed block structure has a greater effect on success. Therefore, a model has been proposed that can be trained and run for Covid19 classification on low-equipped systems.

The following section two of the study presents studies in the literature in general. In section three, ResNet models that are widely used in the literature and the model proposed in the study are shared. In section four, the experimental study is described in detail. In section five, the findings and results of the experimental study are presented. In section six, the results of the study are evaluated and information about future studies is presented.

2. Literature

Researchers have conducted many experimental and theoretical studies to detect diseases of the upper respiratory tract due to the global pandemic in the 21st century [18]-[21]. Among these studies, the most popular are DL-based studies. DL-based approaches are also used in medical image analysis due to their success in classification and prediction. Researchers used X-ray and tomography images to detect Covid19, which is a respiratory illness that affects the upper respiratory system. In the literature section of the study, some of the studies performed with X-ray images are presented in detail below.

Chowdhury et al. conducted their study using a dataset of chest X-rays from 423 Covid19 patients, 1485 viral pneumonia patients, and 1579 healthy individuals. The researchers also used data augmentation methods in addition to the existing dataset. In their study, they tested eight different models that are generally preferred in the field of DL. As a result of the study, they emphasized that the ResNet18 and CheXNeT models achieved the highest success in disease detection with an accuracy rate of 99.41% [2]. Additionally, they found that data augmentation methods directly affect the success of the model.

Farooq and Hafeez proposed a new model called COVID-ResNet, which consists of 4 classes using the COVIDx dataset containing 5941 chest X-rays. Using a three-step technique on the ResNet50 architecture, they achieved a 96.23% success rate with the COVID-ResNet model [22]. Kana et al. achieved a 99.0% success rate in detecting Covid19 in their chest X-rays study using ResNet50 [23].

For the detection of pneumonia and Covid19, Keles et al. developed two models in their study called COV19-CNNet and COV19-ResNet. They used viral pneumonia (350), Covid19 (210), and healthy chest X-rays (350) in their study. They achieved 94.28% and 97.61% classification success for the COV19-CNNet and COV19-ResNet models, respectively. In their study, they emphasized that pre-trained models are less successful in medical images. In the two proposed models, they did not use a pre-trained model, taking a different approach from many studies in the literature. In this sense, it is one of the studies that inspired the present paper [24].

Zhang et al. developed COVID34XrayNet, a ResNet19-based model that uses a two-stage transfer learning approach. The developed model was tested on chest X-rays images and succeeded with 91.8% accuracy in Covid19 detection. The highlight of the model is the addition of a feature smoothing layer (FSL) and a feature extraction layer (FEL) to the 32 layers of the ResNet34 model [25]. Rahaman et al. tested 15 different CNN models and achieved the most classification success (89.3%) with VGG-19 [26].

Asnaoui and Chawki used models with different types of architectural structures in their study. They applied DenseNet201, InceptionResNetV2, InceptionV3, ResNet50, MobilenetV2, VGG16 and VGG19 models on the same dataset. They achieved the highest accuracy with InceptionResNetV2 at 92.18% [27]. The use of different types of DL models by Asnaoui and Chawki is one of the points that inspired our study. This is because it is expected that the success results of models with different types of architecture will be quite different from each other. Examining the success results of models with similar architectures is a very important to show the effect of the preferred layer structure in the development of these models on success. Therefore, in this study, the effect of the number of layers on the success of ResNet models with similar architecture is analyzed.

CT images are also frequently preferred in Covid19 detection with DL applications. For this reason, in the next section of the literature, studies consisting of applications in which CT scan images are preferred are presented. Xu et al. designed a classification network using the ResNet18 model to distinguish Covid19 from the influenza A virus on a dataset of 618 CT images. The images in the dataset were classified by segmentation. In their study, they achieved an accuracy rate of 86.7% [28]. Zheng et al. proposed a CNN-based 3D model named DeCovNet. In their proposed model, they used a total of 630 CT images obtained on different dates. The researchers also used data augmentation techniques to train their proposed model. They detected Covid19 disease using the model they developed and CT images. The performance of the model they developed was measured using the ROC AUC metric and they obtained a value of 0.95 [29]. Hu et al. succeeded in detecting Covid19 disease with 89% accuracy using a weakly supervised DL model with data obtained from CT images. In their study, unlike other studies in the literature, they were able to achieve a higher accuracy rate in disease detection by determining the exact location of the lesions or inflammation caused by Covid19 [30]. Li et al. developed a 3D DL model called COVNet for the detection of Covid19. In their model, they used a dataset of 4352 chest CT images from 3322 patients. With the model they developed using the ResNet50 backbone, the images were first pre-processed. Then, using a UNet-based segmentation method, the infected region was detected from the lung region and classification was performed. With the COVNet model, they obtained AUC values of 0.96, 0.95, and 0.98 for the detection of Covid19, pneumonia, and healthy individuals, respectively [31]. Song et al. developed the DRENet model including VGG16, DenseNet and ResNet models to detect Covid19 causing pneumonia, and localize the main lesions. With the model developed, they achieved a 93% accuracy rate in the classification of CT images obtained from Covid19, healthy individuals and pneumonia [32]. Shah et al., in their study using 738 CT images, suggested a DL model called CTnet10 with an accuracy rate of 82.1%. CTnet10 is compared with DenseNet-169, VGG-16, ResNet-50, InceptionV3, and VGG-19 models in the literature. As a result of the comparison, they determined that although the proposed model has a lower accuracy rate compared to other models, the model has the least duration for training and testing. After the comparison, it is observed that the CTnet10 has a lower accuracy rate than the other models. However, the CTnet10 was found to have the shortest training and testing duration compared to the duration required for training and testing other models [33]. This situation shows that evaluating the proposed models by the success rate alone may not be sufficient. For this reason, success rates and training times were also taken into account in the development of the CTnet10 in the article.

As can be seen from these studies in the literature, it is necessary to develop models that can work with maximum accuracy, especially in minimum training duration [34]. To fill this gap in the literature, a new DL model called 3BResNet has been proposed.

3. Methods

In this section, the general layer structure of CNN-based models, which are commonly used among DL models, the ResNet models used in the study, and the 3BResNet DL model inspired by these models are presented.

3.1. CNN's Basic Layers

CNNs are DL algorithms that usually use two-dimensional images as input and perform convolution with filters to extract features from the image [34]. CNNs are designed to isolate visual components and reduce images to lower dimensions while preserving the essential features of the image [25]. CNN is likened to traditional ANNs, especially because of the structure of its last layer. The determination of the features used in ANN models is usually done by the designer. In CNNs, on the other hand, this structure is different from traditional ANNs. Because the system performs the feature extraction process with the filters used in CNNs. For this reason, it is used as a very popular DL model in the literature [35]. A classical CNN model usually has three different types of layers. These are convolution, pooling, and fully connected layers. These layers are briefly summarized below.

3.1.1. Convolution Layer

One of the most fundamental parts of the CNN architecture is the convolution layer. In general, it performs automatic feature extraction with the filters used during forward propagation. The filter structure used at this stage also constitutes the basic structure of the CNN model. Thanks to the convolution layer, new feature maps are created over the two-dimensional data from the previous layer. This process repeats as many times as the number of convolution blocks added one after the other [36], [37].

3.1.2. Pooling Layer

The overall purpose of the pooling layer is to reduce the number of parameters and the computational complexity of the model. For this, it gradually reduces the representation size [35],[38]. The pooling is usually done by applying filters of different sizes. These filters can be 2x2, 3x3, ..., nxn in size. The most common types of used pooling methods are max, min, and mean pooling. Mean pooling reduces the input size by averaging the pixel values within the pooling region. Max-pooling, on the other hand, reduces the input size by taking the largest value within a pooling zone. This layer increases the learning capacity of the network in the feature extraction process and helps to learn the features of the data [39].

3.1.3. Fully Connected Layer

The fully connected layer is often employed as the output layer at the end of CNN models. Gives the latest output values of CNN models [25]. The feature maps originating from the final convolution or other layers are transformed into a one-dimensional array and passed on to the fully connected layer. In the fully connected layer, each input value is bound to a weighting factor. The number of outputs in the fully connected layer usually contains as many nodes as the number of classes. In the literature, a non-linear (ReLU) activation function is also used after each fully connected layer [36].

3.2. Resnet Models

There is a general belief that more layers should be used in CNN models to improve performance. However, increasing the depth, that is, the number of layers, can cause various problems such as gradient burst or disappearance [40]. The ResNet architecture was developed to overcome these problems. This architecture has become a remarkable architecture in the computer vision sector, winning first awards in the ImageNet Large Scale Visual Recognition Challenge (ILSVRC, 2015) and Microsoft Common Objects in Context (MS COCO, 2015) competitions in 2015 [41].

ResNet models use residual blocks in their layers. These blocks are used to improve the performance of deep networks [42]. Residual blocks possess a general structure that establishes a connection between the input of the layer and the output of the next layers. This structure is shown in detail in Figure 1.

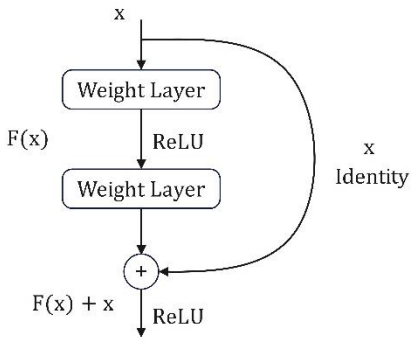

Figure 1. Residual block structure [41]

In Figure 1, x and F(x) refer to the input value of the first layer and the output value of the next layer, respectively. The ReLU between the two layers is the activation function used to reduce the values at the output of the first layer to the desired range [43]. The residual blocks shown in Figure 1 are used to prevent the new values obtained as a result of the convolution process from changing excessively compared to the initial values. Therefore, new ResNet models were developed using different numbers of residual blocks and convolution values. In these architectures, although input images of different sizes can be used, resizing is performed at the input of the models to reduce the images to the appropriate size for the model. This study is based on the ResNet18, ResNet34, ResNet50, ResNet101, ResNet152, and ResNet202 models commonly used in the literature. In these models, five main convolution layers are used: conv1, conv2, conv3, conv4, and conv5 [41]. The content and number of filters used in these layers can be different from each other. The layers of the models used in the study, the blocks belonging to these layers, the matrices used in these blocks and their output dimensions are presented in detail in Table 1.

Table 1. ResNet model family architecture [41]

Layer Name	Output Size	18layer	34layer	50layer	101layer	152layer
conv1	112x112	7x7, 64, stride 2				
conv2x	56x56	3x3 max pool, stride 2				
		$2x\begin{bmatrix}3x3,64\\3x3,64\end{bmatrix}$	$3x\begin{bmatrix}3x3,64\\3x3,64\end{bmatrix}$	$3x\begin{bmatrix}1x1,64\\3x3,64\\1x1,256\end{bmatrix}$	$3x\begin{bmatrix}1x1,64\\3x3,64\\1x1,256\end{bmatrix}$	$3x\begin{bmatrix}1x1,64\\3x3,64\\1x1,256\end{bmatrix}$
conv3x	28x28	$2x\begin{bmatrix}3x3,128\\3x3,128\end{bmatrix}$	$4x\begin{bmatrix}3x3,128\\3x3,128\end{bmatrix}$	$4x\begin{bmatrix}1x1,128\\3x3,128\\1x1,512\end{bmatrix}$	$4x\begin{bmatrix}1x1,128\\3x3,128\\1x1,512\end{bmatrix}$	$8x\begin{bmatrix}1x1,128\\3x3,128\\1x1,512\end{bmatrix}$
conv4x	14x14	$2x\begin{bmatrix}3x3,256\\3x3,256\end{bmatrix}$	$6x\begin{bmatrix}3x3,256\\3x3,256\end{bmatrix}$	$6x\begin{bmatrix}1x1,256\\3x3,256\\1x1,1024\end{bmatrix}$	$23x\begin{bmatrix}1x1,256\\3x3,256\\1x1,1024\end{bmatrix}$	$36x\begin{bmatrix}1x1,256\\3x3,256\\1x1,1024\end{bmatrix}$
conv5x	7x7	$2x\begin{bmatrix}3x3,512\\3x3,512\end{bmatrix}$	$3x\begin{bmatrix}3x3,512\\3x3,512\end{bmatrix}$	$3x\begin{bmatrix}1x1,512\\3x3,512\\1x1,2048\end{bmatrix}$	$3x\begin{bmatrix}1x1,512\\3x3,512\\1x1,2048\end{bmatrix}$	$3x\begin{bmatrix}1x1,512\\3x3,512\\1x1,2048\end{bmatrix}$
	1x1	average pool, 1000-d fc, softmax				
FLOPs		1.8 x 109	3.6 x 109	3.8 x 109	7.6 x 109	11.3 x 109

In the ResNet models, 64 filters of size 7x7 are used in the conv1 convolution layer in all models to quasi the size of the input images. In the conv2 convolution layer, a 3x3 pooling layer is first used for data size reduction. As a result of this process, the size of the data is quasi-ed again. For the remaining operations of the conv2 convolution layer and for operations in other convolution layers, different numbers and sizes of filters are used according to different ResNet models. In the final stage, all outputs are converted into a single vector using the global mean pooling layer. This vector is then sent to the classification layer.

ResNet models have some disadvantages in themselves. Analyzing the FLOPs values presented in Table 1, it is seen that the processing capacity directly increases with increasing the number of layers. When the layer structure in the ResNet18 and ResNet152 models is analyzed, there is approximately six times the computational cost between both models. However, when both models are compared on a similar dataset, the ratio of the accuracy values obtained, and the ratio of the computational cost values cannot be obtained the same. Therefore, when evaluating the performance of the models, they also need to be evaluated in terms of computational cost and training time. Based on this point, this study aims to develop models with less training time.

3.3. Proposed Model

In the developed model, unlike the classical residual blocks used in ResNet models, the block structure shown in Figure 2 is used. In classical residual blocks, there may be anomalous differences between the input data and the output data obtained at the end of the block. Therefore, in the last part of the classical residual block, the initial input data and the final data obtained after the convolution operations are summed with each other. However, if there are small details or small changes between pixels in the images used, these attributes can be lost in classical residual blocks. The loss or inability to obtain these features can cause irreversible problems, especially in healthcare studies using CT-based images. Therefore, in this study, a new structure for the residual blocks is proposed. The 3BResNet residual block structure is shown in detail in Figure 2.

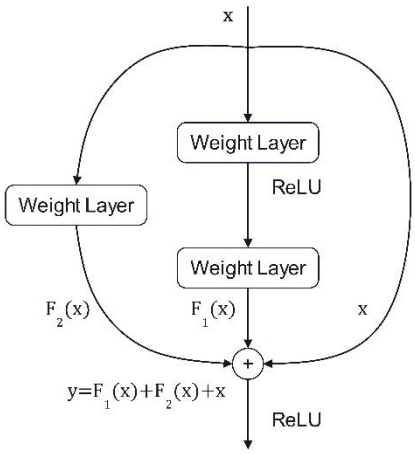

Figure 2. Proposed residual block structure

Data from 3 different branches are combined in the residual block structure proposed in Figure 2. Due to the use of data from 3 branches in the residual block structure, the proposed model is named 3BResNet. In this structure, the data of the first branch represent the input data (x), the data from the second branch represent the data obtained as a result of the sequential convolution operation F1 (x), and the data from the third branch represent the data obtained as a result of the single convolution operation F2 (x). The value denoted by y represents the output of the proposed residual block structure. The mathematical expression of the performed operation is presented in Equation 1.

$$y = (x) + F_1(x) + F_2(x) \quad (1)$$

Due to the structure presented in Equation 1, sudden and large changes between the first image and the last image are prevented, and small details in the image can be captured. Using the proposed residual block, a new 14-layer architecture was created as shown in Figure 3 and Table 2. As it can be understood from this architecture, fewer convolution layers are used than the ResNet18, ResNet34, ResNet50, ResNet101, ResNet152, and ResNet202 models in the literature.

Table 2. 3BResNet architecture

Layer Name	Output Size	14-layer
conv1	112 x 112	7 x 7, 64, stride 2
conv2	56 x 56	[3 x 3], max pool, stride 2
		$\begin{bmatrix} 3x3, 64 \\ 3x3, 64 \end{bmatrix} x2$, stride 1
conv3	28 x 28	$\begin{bmatrix} 3x3, 128 \\ 3x3, 128 \end{bmatrix}$, stride 2 / stride 1
		$\begin{bmatrix} 3x3, 128 \\ 3x3, 128 \end{bmatrix}$, stride 1 / stride 1
conv4	14 x 14	$\begin{bmatrix} 3x3, 256 \\ 3x3, 256 \end{bmatrix}$, stride 2 / stride 1
		$\begin{bmatrix} 3x3, 256 \\ 3x3, 256 \end{bmatrix}$, stride 1 / stride 1
	1x1	average pool, 1000-d fc, softmax
FLOPs		$1{,}9x10^9$

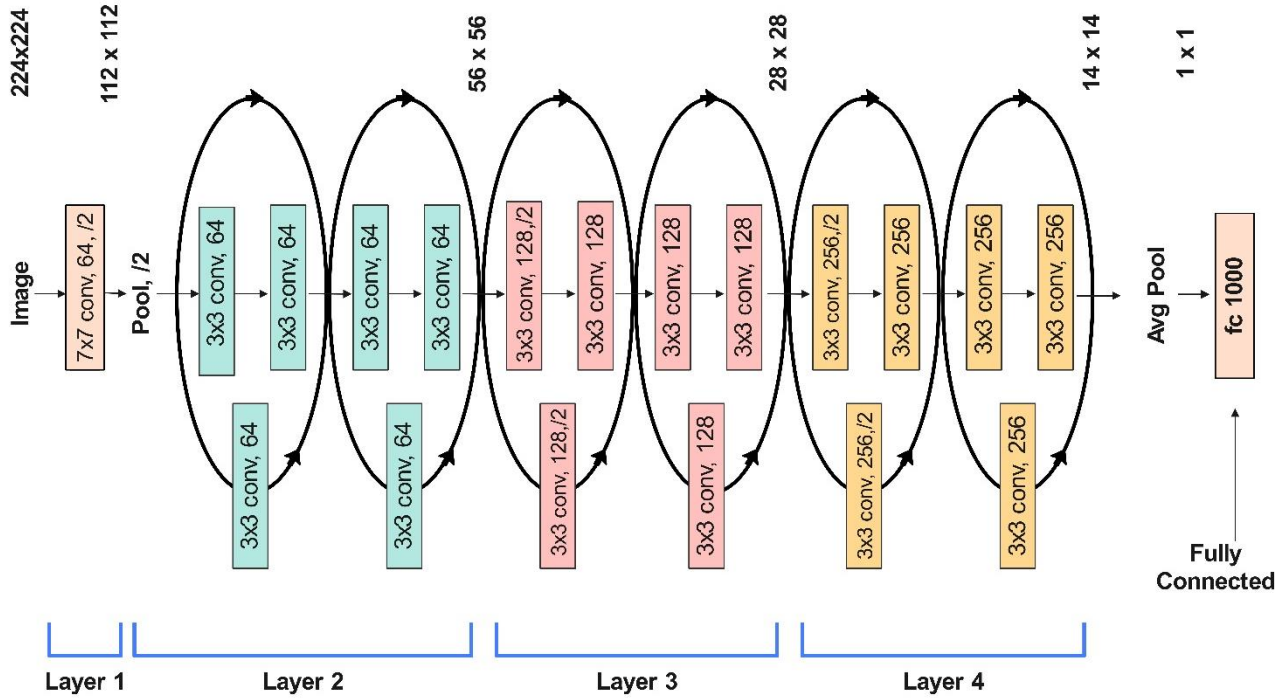

Figure 3. Architecture of the 3BResNet model

4. Experimental Study

The experimental study carried out consists of 4 steps as shown in Figure 4. These steps are data pre-processing, model selection, implementation, and testing. The results of the experimental study are compared in Table 5 with the results of other studies in the literature using the same dataset.

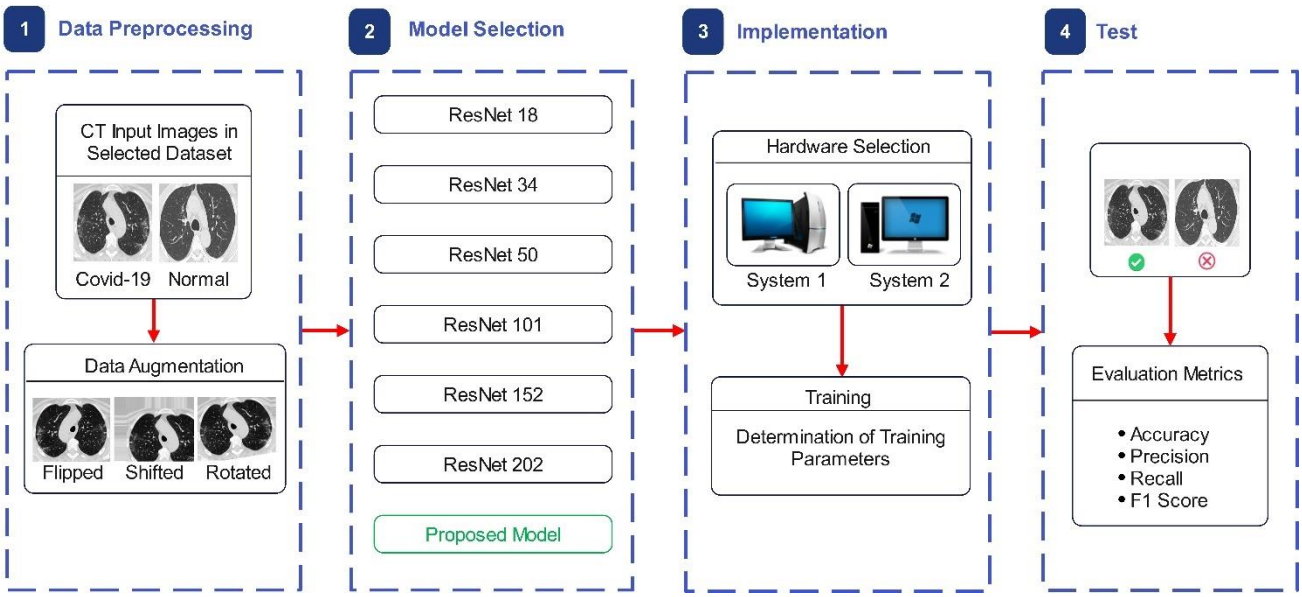

Figure 4. Experimental study diagram

4.1. Data Pre-Processing

This section of the study, information about the dataset used is given and the steps followed for data augmentation are presented.

4.1.1. Selected Dataset

Within the scope of the study, the SARS-CoV-2 CT dataset, which is used in many different studies in the literature, was used to evaluate the performance of the ResNet models and the 3BResNet model together with other studies in the literature [44]. The dataset used was obtained from CT images of patients in hospitals in Sao Paulo, Brazil, by Soares et al., to be used in the diagnosis of SARS-CoV-2 (COVID19) infection. There are 1252 positive and 1230 negative CT images in the dataset. The examples of positive and negative Covid19 chest CT scans shown in Figure 5.

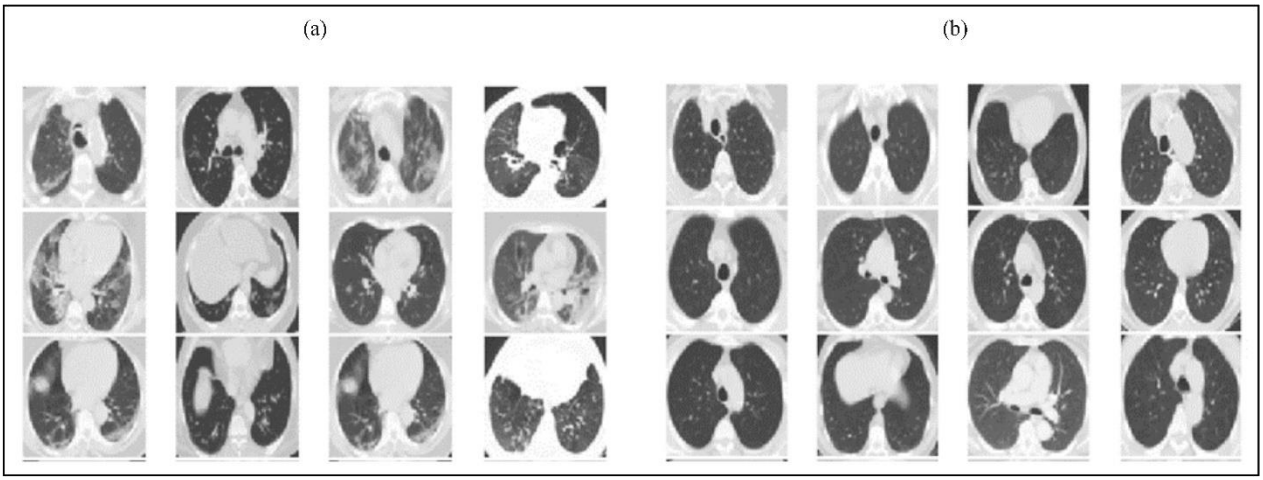

Figure 5. a) Positive COVID19 chest CT scans b) Negative COVID19 chest CT scans

4.1.2 Data Augmentation Processing

Data augmentation processing is a strategy that aims to generate more samples by applying different transformations to the available training data [45]. By ensuring that the network encounters different data in each training round, the aim is to prevent the problem of overfitting and, accordingly, increase the generalization performance of the model. Deep neural networks need high-quality training examples to get accurate results. However, biomedical image datasets often contain fewer images than publicly available image datasets. Many biomedical datasets, including the dataset used in this study, contain fewer than 10,000 images.

For this reason, three different data augmentation techniques were applied to increase the number of images in the study. The data augmentation methods preferred in the study are image rotation, image shift, and flip. 90-degree angles were used for image rotation. In the image shift process, 0.2, 0.4, and 0.6 values are preferred as the shift value, and horizontal flipping is preferred in the flipping process. As the images obtained by these methods are variants of the original images and have similar patterns, they can be considered reliable data. An example of the images obtained because of the data augmentation process is shown in Figure 6.

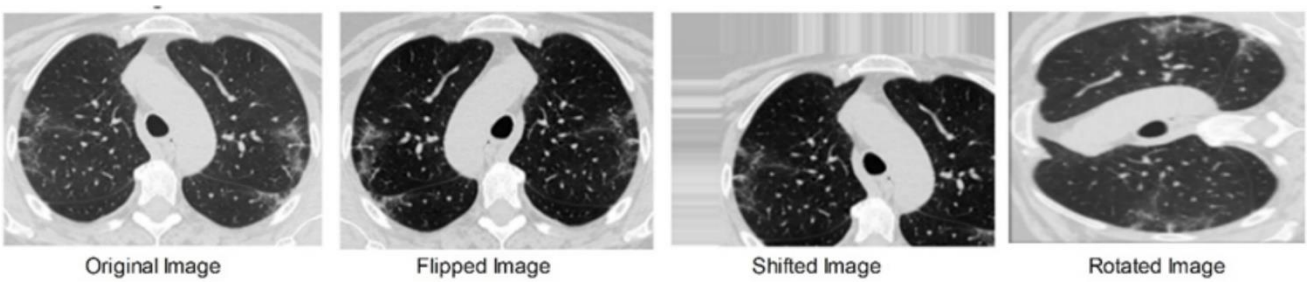

Figure 6. Examples of augmented images

In the study, the augmented data were separated into two groups as 80% training and 20% test data according to the cross-validation 5 value. The images in the dataset used in this study have different dimensions. For this reason, all images were resized to 224x224 to be suitable for the input of the models to be used in the next stages of the study.

4.2. Model Selection

The general structure of the model proposed in the study is presented in detail in Section 3.3. The DL models ResNet202, ResNet34, ResNet152, ResNet101, ResNet150, and ResNet18, which are widely used in the literature with similar parameters, are other preferred models in the study. The number of layers and the contents of these models used are discussed in detail in Section 3.3. To compare the performance of ResNet models, it is very important to use the same dataset and train with the same training parameters. As can be seen in Figure 4, whichever model is selected in the experimental study, the whole system is run on that model and results are produced. This step is repeated to train and test each model.

4.3. Implementation

In this step of the study, the hardware options and training parameters used in the experimental study are presented.

4.3.1. Hardware

To measure the effect of different DL models applied in the study on different hardware, it was aimed at performing training and testing processes on two different hardware systems. For this reason, detailed specifications of the hardware used in the study are shown in Table 3.

Table 3. Details of hardware and software used

	Hardware			Software		
	CPU	**GPU**	**RAM**	**Operating System**	**Programming Language**	**Library**
System 1	Intel Core i7 7500U 2.70GHz 2 Core	Intel HD Graphics 620	8 GB	Windows 10 Enterprise 64-bit	Python 3.8	TensorFlow v2.11.0
System 2	Intel Core i7 10750H 2,60 GHz 16 Core	NVIDIA GeForce GTX 1650 TI	64 GB	Windows 10 Enterprise 64-bit	Python 3.8	TensorFlow v2.11.0

4.3.2. Training

In this study, the training parameters of the ResNet models were determined taking into account the GPU memory limit of the system hardware to be used and the size of the data stacks to be used during training. Therefore, the batch size value is 64. A slow value is preferred for the learning rate of the network. Therefore, 0.001 was used as the learning parameter. Adam optimizer is preferred to optimize the parameters of the system. All models were trained using 500 epochs. In the study, the data were divided into two groups, training, and testing, according to the cross-validation value of 5. Data separated according to this value was used in the training phase. The metrics used to measure training and testing performance are presented in detail in section 4.4.

4.4. Evaluation Metrics

In order to analyze the performances of the DL architectures used in the study and the 3BResNet model, the confusion matrix, which is widely used in classification applications in the literature, was used [46]. Confusion matrix is a construct designed to evaluate the prediction accuracy of classification algorithms. With the Confusion matrix, information about the errors of the classification models used, the types of errors, and the performance of the model, in general, can be obtained.

The confusion matrix has four different values. These are True Positive (TP), True Negative (TN), False Positive (FP), and False Negative (FN). Sample values that the system predicts positively and that are actually positive are denoted by TP. Sample values that the system predicts negatively and are

actually negative are denoted by TN. Sample values that the system predicts as positive but are actually negative are represented by FP. Sample values that the system predicts negatively but are actually positive are compared with FN. Expressed. Equation 2-5 evaluates the overall performance of the system using these parameters.

$$\text{Accuracy;}\ \frac{(TN+TP)}{(TP+TN+FP+FN)} \quad (2)$$

$$\text{Precision;}\ \frac{(TP)}{(FP+TP)} \quad (3)$$

$$\text{Recall;}\ \frac{(TP)}{(FN+TP)} \quad (4)$$

$$\text{F1 Score;}\ 2x\left(\frac{Recall * Precision}{Recall + Precision}\right) \quad (5)$$

The criterion used to evaluate the success of the classification model is defined as accuracy. This metric, presented in Equation 2, is expressed as the ratio of the number of correctly classified samples to the total number of samples. The criterion used to evaluate how many of the positive classes predicted by the classification model are actually positive is defined as precision. This metric, presented in Equation 3, is calculated by dividing the number of correct positive predictions by the number of all positive predictions in the matrix. The criterion used to evaluate how accurately the classification model classifies true positive samples is defined as sensitivity. This metric, presented in Equation 4, is calculated by dividing the number of true positive predictions in the matrix by the number of true positive samples. The F1 Score presented in Equation 5, on the other hand, expresses the balance between the accuracy and precision of the model. It is calculated as the harmonic mean of the accuracy and precision criteria.

5. Result and Discussion

The results of the experimental studies and discussions are shared in detail in this section. The results are then compared with other previous studies in the literature using the same dataset.

5.1. Performance Analysis

Despite the difficulties in diagnosing upper respiratory tract infections, there is a trend toward DL models due to the high performance of machine learning methods [47]. For this reason, DL models were preferred in the study. All preferred models and the 3BResNet model were tested separately on the same data set and performance evaluation was made. Due to the preferred dataset, there has been a classification as positive or negative for Covid19.

The training and testing procedures for all models used in this study were carried out using System 2, which is presented in Table 3. In the training phase of the study, the accuracy, precision, sensitivity, F1 score, training duration, and flops obtained separately for all models are presented in detail in Table 4.

Table 4. Analysis results

Model	Flops	Accuracy	Precision	Recall	F1 Score	Duration
ResNet18	$1.8x10^9$	0.94	0.94	0.96	0.95	610 sec
ResNet34	$3.6x10^9$	0.95	0.98	0.92	0.95	868 sec
ResNet50	$3.8x10^9$	0.95	0.92	0.96	0.94	1361 sec
ResNet101	$7.6x10^9$	0.95	0.96	0.95	0.95	2057 sec
ResNet152	$11.3x10^9$	0.90	0.95	0.87	0.91	2842 sec
ResNet202	$14.8x10^9$	0.92	0.95	0.90	0.93	3732 sec
Proposed Model(3BResNet)	$1.9x10^9$	0.97	0.96	0.98	0.97	675 sec

Although in the literature thought that increasing the number of layers used in CNN-based models will increase success, the opposite is found in this study. When the training results of the system in Table 4 are analyzed, it is seen that the accuracy does not change at the same rate and direction with the number of layers. In addition, it was found that the number of parameters used, and

the time required to train the models increased due to the increase in the number of layers. It has been observed that the accuracy obtained from ResNet152 and ResNet202 models, which have a greater number of layers, is lower than other models.

In this study, inspired by ResNet models, the 3BResNet model achieved a classification success much superior to other ResNet models, reaching an accuracy value of 0.97, despite reducing the number of layers and modifying its structure. The residual block structure used in the 3BResNet model has been found to shorten the training time and increase the success rate.

When the training time and the number of parameters of all models were examined, it was determined that the proposed model completed the training process faster than all other ResNet models except ResNet18. In the 3BResNet model, more parameters are used than the number of parameters used in ResNet18. This is due to the increase of convolution operations in the block structure of the 3BResNet model. As a result of this, the training duration of the ResNet18 model was shorter than that of the 3BResNet model.

In addition, the 3BResNet model was trained and tested with the lower hardware System 1 presented in Table 3. Training of the 3BResNet model with System 1 was completed in 2342 seconds. On the other hand, the same model was trained with System 2 for 675 seconds. Thus, the low-equipped system was compared with the high-equipped system, and it was determined that the 3BResNet model could also work in low-equipped systems by compromising the training time. When the results are examined in general, it is seen that the training time of the 3BResNet model is much shorter than the training times of the ResNet152 and ResNet202 models.

5.2. Comparison With State of The Art

In order to present a realistic evaluation of the 3BResNet model and other ResNet models used in the study, a comparison was made with the state of the art (SOTA) latest technology studies using the same data set in the literature. The comparison made is presented in Table 5 in detail. In the evaluation, it is detected that especially the Inception ResNet model performs lower than many studies in the literature. The success rates of the ResNet models used in the study and the VGG and DenseNet models are seen to be close to each other. The 3BResNet model showed a 97% classification success. This result shows that the 3BResNet model has the potential to compete with other models in the existing literature.

Table 5. Comparison with the SOTA in literature

References	Pre-trained model	Accuracy
[48]	VGG-16	0.94
[49]	DenseNet201	0.96
	VGG-16	0.95
	ResNet 152V2	0.94
	Inception ResNet	0.90
[13]	DenseNet201	0.97
	VGG-16	0.94
	ResNet50V2	0.96
	MobileNet	0.95
[50]	VGG-19	0.94
[51]	VGG-19 with LR	0.94
	VGG-19 with KNN	0.94
	VGG-16 with LR	0.94
	VGG-16 with KNN	0.94
[52]	ResNet50	0.95
Our Study	ResNet18	0.94
	ResNet34	0.95
	ResNet50	0.95
	ResNet101	0.95
	ResNet152	0.90
	ResNet202	0.92
	Proposed(3BResNet)	0.97

6. Conclusion

The ResNet models used in the literature are open to improvement and new models can be developed by adding different layers. However, in DL models, semantic gaps can occur when high depth levels are reached. There may be different reasons for these semantic gaps. Although increasing the number of layers in ResNet models is done to increase performance, this may produce low performance

results depending on the dataset. For this reason, a new model called 3BResNet with a new layer and block structure is proposed in this study, inspired by the ResNet models in the literature. In the 3BResNet model, instead of increasing the number of layers, the residual block structure used in ResNet models is modified, and the number of layers is reduced to 14 layers.

The 3BResNet model is also aimed to solve the gradient vanishing and explosion problem, which is commonly encountered in ResNet models in the literature. To objectively evaluate the performance, different ResNet models were also trained and tested using the same dataset.

The confusion matrix, which is commonly used in the literature, was used in the training and testing processes. In addition, two different hardware configurations were also created to measure the performance of the system at different hardware levels. The 3BResNet model can run on a high-equipped level as well as on a much lower-equipped level. Therefore, the proposed model is considered a suitable solution to deal with hardware problems commonly encountered in DL models. With this study, a method that can be widely used at all levels of hardware during epidemic periods, such as a pandemic, has been developed.

With the 3BResNet model proposed in the study, a more successful result was obtained than other ResNet models in the literature, reaching an accuracy rate of 0.97 in classifying people infected with Covid19. In addition, the training time of the model was completed in 675 seconds. This time is much less than the ResNet models used in the study. Training of the 3BResNet model on machines of different hardware levels has also been tested. As a result of the test, it has been seen that training can be performed on systems with low hardware levels. System 1 was used as an example of a low-equipped system in the study. The training process on System 1 was completed in 2342 seconds. It has been observed that the proposed model can be trained on a low-equipped system, with some sacrifice of training time. In light of the results obtained, it was determined that the 3BResNet model performed better than the ResNet models used in the study.

Considering the success of the proposed model in image classification, it is anticipated that it can be applied not only to medical image datasets, but also to various datasets from different fields. It has been concluded that the focus of the studies planned to be carried out on the basis of ResNet models in the future is to develop models that can provide higher success with shorter training time by developing different block structures, rather than increasing the number of layers. This approach will provide a different perspective to overcome current limitations and achieve higher accuracy rates. The model proposed in the study is capable of contributing to future studies to make the education process faster and more efficient.

Contributions of the authors

The authors confirm that the contribution is equally for this paper.

Conflict of Interest Statement

There is no conflict of interest between the authors.

Statement of Research and Publication Ethics

The study is complied with research and publication ethics.

References

[1] A. A. Ardakani, A. R. Kanafi, U. R. Acharya, N. Khadem, ve A. Mohammadi, "Application of deep learning technique to manage COVID-19 in routine clinical practice using CT images: Results of 10 convolutional neural networks", *Comput Biol Med*, vol. 121, Haz. 2020, doi: 10.1016/j.compbiomed.2020.103795.

[2] M. E. H. Chowdhury *vd.*, "Can AI Help in Screening Viral and COVID-19 Pneumonia?", *IEEE Access*, vol. 8, pp. 132665-132676, 2020, doi: 10.1109/ACCESS.2020.3010287.

[3] Z. hui Chen, S. ping Wan, ve J. ying Dong, "An integrated interval-valued intuitionistic fuzzy technique for resumption risk assessment amid COVID-19 prevention", *Inf Sci (N Y)*, vol. 619, pp. 695-721, Oca. 2023, doi: 10.1016/j.ins.2022.11.028.

[4] X. Li, C. Li, ve D. Zhu, "Covid-mobilexpert: On-device covid-19 screening using snapshots of chest x-ray", *arXiv preprint arXiv:2004.03042*, 2020.

[5] Çalışkan, A. (2023). "Diagnosis of malaria disease by integrating chi-square feature selection algorithm with convolutional neural networks and autoencoder network", *Transactions of the Institute of Measurement and Control*, vol. 45, no. 5, pp. 975-985. https://doi.org/10.1177/01423312221147335.

[6] M. P. Cheng *vd.*, "Diagnostic Testing for Severe Acute Respiratory Syndrome–Related Coronavirus 2", *Ann Intern Med*, vol. 172, no 11, pp. 726-734, Nis. 2020, doi: 10.7326/M20-1301.

[7] X. He *vd.*, "Sample-efficient deep learning for COVID-19 diagnosis based on CT scans", in *IEEE Transactions on Medical Imaging*, p. 10, 2020. doi: 10.1101/2020.04.13.20063941.

[8] T. B. Chandra, K. Verma, B. K. Singh, D. Jain, ve S. S. Netam, "Coronavirus disease (COVID-19) detection in Chest X-Ray images using majority voting based classifier ensemble", *Expert Syst Appl*, vol. 165, p. 113909, 2021, doi: https://doi.org/10.1016/j.eswa.2020.113909.

[9] A. Bernheim et al., "Chest CT findings in coronavirus disease 2019 (COVID-19): Relationship to duration of infection", *Radiology*, vol. 295, no 3, pp. 200463, 2020. doi: 10.1148/radiol.2020200463.

[10] O. Gozes *et al.*, "Rapid AI Development Cycle for the Coronavirus (COVID-19) Pandemic: Initial Results for Automated Detection & Patient Monitoring using Deep Learning CT Image Analysis", 2020, [Çevrimiçi]. Erişim adresi: http://arxiv.org/abs/2003.05037

[11] R. Chelghoum, A. Ikhlef, A. Hameurlaine, and S. Jacquir, "Transfer learning using convolutional neural network architectures for brain tumor classification from MRI images", in *IFIP Advances in Information and Communication Technology*, Springer International Publishing, 2020, pp. 189-200. doi: 10.1007/978-3-030-49161-1_17.

[12] S. Metlek, "A new proposal for the prediction of an aircraft engine fuel consumption: a novel CNN-BiLSTM deep neural network model", *Aircraft Engineering and Aerospace Technology*, vol. 95, no 5, pp. 838-848, 2023, doi: 10.1108/AEAT-05-2022-0132.

[13] A. Halder and B. Datta, "COVID-19 detection from lung CT-scan images using transfer learning approach", *Mach Learn Sci Technol*, vol. 2, no 4, p. 0450013, 2021. doi: 10.1088/2632-2153/abf22c.

[14] M. Usman, T. Zia, and A. Tariq, "Analyzing transfer learning of vision transformers for interpreting chest radiography", *J Digit Imaging*, vol. 35, no. 6, pp. 1445-1462, 2022.

[15] C. Srinivas et al., "Deep transfer learning approaches in performance analysis of brain tumor classification using MRI images", *J Healthc Eng*, vol. 2022, 2022.

[16] H. Aljuaid, N. Alturki, N. Alsubaie, L. Cavallaro, and A. Liotta, "Computer-aided diagnosis for breast cancer classification using deep neural networks and transfer learning", *Comput Methods Programs Biomed*, vol. 223, p. 106951, 2022.

[17] M. Aly and N. S. Alotaibi, "A novel deep learning model to detect COVID-19 based on wavelet features extracted from Mel-scale spectrogram of patients' cough and breathing sounds", *Inform Med Unlocked*, vol. 32, p. 101049, 2022, doi: https://doi.org/10.1016/j.imu.2022.101049.

[18] L. K. Butola, R. Ambad, P. K. Kute, R. K. Jha, A. D. Shinde, and W. DMIMS, "The pandemic of 21st century-COVID-19", *Journal of evolution of medical and dental Sciences-JEMDS*, vol. 9, no 39, pp. 2913-2918, 2020.

[19] Y. Zhao, B. R. Dong, and Q. Hao, "Probiotics for preventing acute upper respiratory tract infections", *Cochrane Libr*, no. 8, 2022, doi: 10.1002/14651858.CD006895.pub4.

[20] A. Bianco, F. Licata, C. G. A. Nobile, F. Napolitano, ve M. Pavia, "Pattern and appropriateness of antibiotic prescriptions for upper respiratory tract infections in primary care paediatric patients", *Int J Antimicrob Agents*, vol. 59, no 1, p. 106469, 2022. doi: https://doi.org/10.1016/j.ijantimicag.2021.106469.

[21] A. W. Bartlow *vd.*, "Comparing variability in diagnosis of upper respiratory tract infections in patients using syndromic, next generation sequencing, and PCR-based methods", *PLOS Global Public Health*, vol. 2, no 7, pp. e0000811, 2022. https://doi.org/10.1371/journal.pgph.0000811

[22] M. Farooq and A. Hafeez, "Covid-resnet: A deep learning framework for screening of covid19 from radiographs", *arXiv preprint arXiv:2003.14395*, 2020.

[23] E. B. G. Kana, M. G. Z. Kana, A. F. D. Kana, and R. H. A. Kenfack, "A web-based Diagnostic Tool for COVID-19 Using Machine Learning on Chest Radiographs (CXR)", *medRxiv*, s. 2020.04.21.20063263, 2020. doi: 10.1101/2020.04.21.20063263.

[24] A. Keles, M. B. Keles, and A. Keles, "COV19-CNNet and COV19-ResNet: diagnostic inference Engines for early detection of COVID-19", *Cognit Comput*, pp. 1-11, 2021.

[25] R. Zhang *et al.*, "COVID19XrayNet: A Two-Step Transfer Learning Model for the COVID-19 Detecting Problem Based on a Limited Number of Chest X-Ray Images", *Interdiscip Sci*, vol. 12, no 4, pp. 555-565, 2020. doi: 10.1007/s12539-020-00393-5.

[26] M. M. Rahaman *et al.*, "Identification of COVID-19 samples from chest X-Ray images using deep learning: A comparison of transfer learning approaches", *J Xray Sci Technol*, vol. 28, no. 5, pp. 821-839, 2020, doi: 10.3233/XST-200715.

[27] K. El Asnaoui and Y. Chawki, "Using X-ray images and deep learning for automated detection of coronavirus disease", *J Biomol Struct Dyn*, vol. 39, no 10, pp. 3615-3626, 2021.

[28] X. Xu *et al.*, "A deep learning system to screen novel coronavirus disease 2019 pneumonia", *Engineering*, vol. 6, no 10, pp. 1122-1129, 2020.

[29] C. Zheng *et al.*, "Deep Learning-based Detection for COVID-19 from Chest CT using Weak Label", *IEEE Trans Med Imaging*, pp. 1-13, 2020, doi: 10.1101/2020.03.12.20027185.

[30] S. Hu *et al.*, "Weakly supervised deep learning for covid-19 infection detection and classification from ct images", *IEEE Access*, vol. 8, pp. 118869-118883, 2020.

[31] L. Li *et al.*, "Using Artificial Intelligence to Detect COVID-19 and Community-acquired Pneumonia Based on Pulmonary CT: Evaluation of the Diagnostic Accuracy", *Radiology*, vol. 296, no 2, pp. E65-E71, Mar. 2020, doi: 10.1148/radiol.2020200905.

[32] Y. Song *et al.*, "Deep learning enables accurate diagnosis of novel coronavirus (COVID-19) with CT images", *IEEE/ACM Trans Comput Biol Bioinform*, vol. 18, no 6, pp. 2775-2780, 2021.

[33] V. Shah, R. Keniya, A. Shridharani, M. Punjabi, J. Shah, and N. Mehendale, "Diagnosis of COVID-19 using CT scan images and deep learning techniques", *Emerg Radiol*, vol. 28, no 3, pp. 497-505, 2021.

[34] S. Metlek, "Forecasting of Dow Jones sukuk index prices using artificial intelligence systems.", *Econ Comput Econ Cybern Stud Res*, vol. 56, no 1, 2022.

[35] K. O'Shea ve R. Nash, "An Introduction to Convolutional Neural Networks", *CoRR*, c. abs/1511.0, 2015, [Çevrimiçi]. Erişim adresi: http://arxiv.org/abs/1511.08458

[36] R. Yamashita, M. Nishio, R. K. G. Do, and K. Togashi, "Convolutional neural networks: an overview and application in radiology", *Insights into Imaging*, vol. 9, no 4. pp. 611-629, 2018. doi: 10.1007/s13244-018-0639-9.

[37] J. Gu *et al.*, "Recent advances in convolutional neural networks", *Pattern Recognit*, vol. 77, pp. 354-377, 2018. doi: 10.1016/j.patcog.2017.10.013.

[38] S. Albawi, T. A. Mohammed, ve S. Al-Zawi, "Understanding of a convolutional neural network", in *2017 International Conference on Engineering and Technology, (ICET)* 2017. doi: 10.1109/ICEngTechnol.2017.8308186.

[39] A. Arı and D. Hanbay, "Bölgesel Evrişimsel Sinir Ağları Tabanlı MR Görüntülerinde Tümör Tespiti", *Gazi Üniversitesi Mühendislik-Mimarlık Fakültesi Dergisi*, vol. 2018, no 18-2, 2018. doi: 10.17341/gazimmfd.460535.

[40] M. Tokmak and A. Kıraç, "Classification of Some Species of Shrikes Family by Convolutional Neural Networks", *Bilge International Journal of Science and Technology Research*, vol. 5, no. 1, pp. 72-79 2021, doi: 10.30516/bilgesci.886291.

[41] K. He, X. Zhang, S. Ren, ve J. Sun, "Deep residual learning for image recognition", in 2016 *IEEE Conference on Computer Vision and Pattern Recognition (CVPR)*, 2016. doi: 10.1109/CVPR.2016.90.

[42] Z. Lu *et al.*, "The classification of gliomas based on a Pyramid dilated convolution resnet model", *Pattern Recognit Lett*, vol. 133, pp. 173-179, 2020, doi: https://doi.org/10.1016/j.patrec.2020.03.007.

[43] Q. A. Al-Haija ve A. Adebanjo, "Breast cancer diagnosis in histopathological images using ResNet-50 convolutional neural network", in 2020 IEEE *International IOT, Electronics and Mechatronics Conference (IEMTRONICS)*, 2020. doi: 10.1109/IEMTRONICS51293.2020.9216455.

[44] E. Soares, P. Angelov, S. Biaso, M. H. Froes, ve D. K. Abe, "SARS-CoV-2 CT-scan dataset: A large dataset of real patients CT scans for SARS-CoV-2 identification", *medRxiv*, s. 2020.04.24.20078584, Oca. 2020, doi: 10.1101/2020.04.24.20078584.

[45] K. Maharana, S. Mondal, ve B. Nemade, "A review: Data pre-processing and data augmentation techniques", *Global Transitions Proceedings*, vol. 3, no 1, pp. 91-99, 2022, doi: https://doi.org/10.1016/j.gltp.2022.04.020.

[46] O. Turk, D. Ozhan, E. Acar, T. C. Akinci, & M. Yilmaz, (2022). "Automatic detection of brain tumors with the aid of ensemble deep learning architectures and class activation map indicators by employing magnetic resonance images," *Z. Med. Phys.*, 2022. https://doi.org/10.1016/j.zemedi.2022.11.010.

[47] S. Siddiqui *vd.*, "Deep Learning Models for the Diagnosis and Screening of COVID-19: A Systematic Review", *SN Computer Science*, vol. 3, no 5, 2022. doi: 10.1007/s42979-022-01326-3.

[48] E. Soares, P. Angelov, S. Biaso, M. H. Froes, ve D. K. Abe, "SARS-CoV-2 CT-scan dataset: A large dataset of real patients CT scans for SARS-CoV-2 identification", *medRxiv*, p. 2020.04.24.20078584, Oca. 2020, doi: 10.1101/2020.04.24.20078584.

[49] A. Jaiswal, N. Gianchandani, D. Singh, V. Kumar, ve M. Kaur, "Classification of the COVID-19 infected patients using DenseNet201 based deep transfer learning", *J Biomol Struct Dyn*, vol. 39, no 15, pp. 5682-5689, 2021, doi: 10.1080/07391102.2020.1788642.

[50] H. Panwar, P. Gupta, M. K. Siddiqui, R. Morales-Menendez, P. Bhardwaj, ve V. Singh, "A Deep Learning and Grad-CAM based Color Visualization Approach for Fast Detection of COVID-19 Cases using Chest X-ray and CT-Scan Images", *Chaos Solitons Fractals*, vol. 140, no. 110190, p. 110190, Ağu. 2020, doi: 10.1016/j.chaos.2020.110190.

[51] S. Gupta, P. Aggarwal, N. Chaubey, and A. Panwar, "Accurate prognosis of Covid-19 using CT scan images with deep learning model and machine learning classifiers", *Indian Journal of Radio &Space Physics*,vol.50, no. 1, pp.19-24, 2021.

[52] K. L. Kohsasih ve B. H. Hayadi, "Classification SARS-CoV-2 Disease based on CT-Scan Image Using Convolutional Neural Network", *Scientific Journal of Informatics*, vol. 9, no 2, pp. 197-204, Kas. 2022, doi: 10.15294/sji.v9i2.36583.